

On the effects of rotation on acoustic stellar pulsations: validity domains of perturbative methods and close frequency pairs

K. D. Burke^{1*}, D. R. Reese^{1,2} and M. J. Thompson^{1,3}

¹*Department of Applied Mathematics, University of Sheffield, Hicks Building, Hounsfield Road, S3 7RH, Sheffield, UK*

²*Observatoire de Paris, LESIA, CNRS UMR 8109, 92195 Meudon, France*

³*High Altitude Observatory, National Center for Atmospheric Research, Boulder, CO 80307*

Accepted ????. Received ???; in original form ???

ABSTRACT

Pulsation frequencies of acoustic modes are calculated for realistic rotating stellar models using both a perturbative and a two-dimensional approach. A comparison between the two yields validity domains which are similar to those previously obtained in Reese, Lignières & Rieutord (2006) for polytropic models. One can also construct validity domains based on polynomial fits to the frequencies from the two-dimensional approach, and these also turn out to be similar, thus further confirming the agreement between the perturbative and two-dimensional approach at low rotation rates. Furthermore, as was previously shown in Espinosa, Pérez Hernández & Roca Cortés (2004), adjacent frequencies in multiplets come close together, thus forming pairs. This phenomena, exclusive to two-dimensional calculations, is shown to be an unlikely explanation of the close frequency pairs observed in δ Scuti stars. A systematic search for all close frequency pairs in the calculated spectrum is also carried out. The number of close frequency pairs is shown to agree with what is expected based on a Poisson distribution, but does not match the number or distribution of close pairs in stars like FG Vir. Furthermore, a lack of close frequency pairs appears at low rotation rates, where frequency multiplets do not overlap. Delta Scuti stars currently reported as having close frequency pairs do not fall in this interval.

Key words: stars: oscillations (including pulsations) – stars: rotation – non-perturbative methods

1 INTRODUCTION

The new space missions, CoRoT and Kepler, are substantially increasing the accuracy with which stellar pulsations are observed. A look at CoRoT's and Kepler's first asteroseismic results shows the progress that has been made in the photometric detection of solar-like oscillations, as well as the substantial increase in the number of detected modes in earlier type stars such as δ Scuti stars (Michel et al. 2008, Kjeldsen et al. 2010). The high duty cycle and the long observational runs (up to 5 months for CoRoT and several years for Kepler) are key factors in this dramatic improvement. As a result, there is a drive on the theoretical side to achieve accurate computations of pulsation frequencies in stellar models. Although a fair amount of success has been achieved in slowly rotating stars, much work is still needed before being able to accurately model pulsation

modes in rapidly rotating stars. This is because at rapid rotation rates, the centrifugal force causes stellar deformation thereby transforming what used to be a one-dimensional eigenvalue problem into one that is two-dimensional. This is all the more problematic as many stars rotate rapidly.

In order to address the effects of rotation, two different methods have been developed. The first is the perturbative method which starts from a non-rotating star and then includes various corrections which model the effects of rotation. These corrections are generally expressed as a power series in terms of the rotation rate which is assumed to be a small parameter. Previous works include Saio (1981), Gough & Thompson (1990) and Dziembowski & Goode (1992) for the second order, and Soufi, Goupil & Dziembowski (1998) and Karami et al. (2005) for the third order. The advantage of this method is that it is computationally less expensive and mode classification is more straightforward, thereby allowing an efficient study of an entire

* E-mail: K.Burke@sheffield.ac.uk

spectrum of pulsation modes for a given model. However this method is only valid for slow rotation rates. The other approach consists in solving directly the two-dimensional eigenvalue system. Previous works which focus on p-modes include Clement (1981), Yoshida & Eriguchi (2001), Espinosa, Pérez Hernández & Roca Cortés (2004), Lignières, Rieutord & Reese (2006) and Lovekin & Deupree (2008). Although computationally more expensive, this method can handle pulsation modes at any rotation rate. A natural question is at what rotation rates does it become necessary to use a two-dimensional approach rather than a perturbative approach.

A number of previous works have focused on answering the above question in the case of acoustic modes. In Reese, Lignières & Rieutord (2006), validity domains were established for third order perturbative methods. The underlying stellar models were polytropic and the perturbative calculations were, in fact, polynomial fits to the non-perturbative¹ frequencies. Later on, Lovekin & Deupree (2008) did comparisons using more realistic models. Once more the perturbative calculations were polynomial fits to the non-perturbative frequencies. Given the larger error bars on the calculations, perturbative calculations were considered to be valid up to higher rotation rates. Other works include Ouazzani et al. (2009) where non-perturbative frequencies were compared with frequencies resulting, this time, from a perturbative analysis rather than a polynomial fit. Furthermore, the effects of avoided crossings were included in the perturbative calculations and shown to improve the agreement with two-dimensional calculations. Finally, Suárez et al. (2010) investigated the effects of perturbative and non-perturbative frequencies of polytropic models on echelle diagrams and various frequency separations. They showed that including avoided crossings in perturbative analysis becomes necessary for correctly predicting the behaviour of the small frequency separation, even at relatively low rotation rates. Nonetheless, a systematic study of the validity of perturbative methods for realistic models is still lacking. Given the accuracy of the new pulsation data coming from the CoRoT and Kepler missions, such a study is needed in order to correctly interpret this data. Therefore, in the present work, we will compare two-dimensional calculations with frequencies resulting from a second order perturbative analysis and establish validity domains similar to those in Reese et al. (2006). These calculations will be carried out for acoustic modes, using realistic stellar models rather than polytropic ones. Furthermore, we will discuss some of the qualitative differences between the two types of calculations.

The next section deals with the stellar models. This is then followed by a description of the perturbative and two-dimensional pulsation calculations. Section 4 compares the results from the two approaches and section 5 deals with close frequency pairs, both within multiplets, and for an entire spectrum. Finally, a discussion concludes the paper.

¹ The term “non-perturbative frequencies” in this context means frequencies based on a two-dimensional calculation, rather than frequencies in which the effects of rotation have been removed.

2 MODELS

Stellar models were created using the Aarhus stellar evolution code, ASTEC (Christensen-Dalsgaard 2008b). The OPAL 1995 opacity tables (Iglesias & Rogers 1996) were used in conjunction with the Kurucz low temperature adjustments (Kurucz 1991), and the Eggleton, Faulkner & Flannery equation of state (Eggleton, Faulkner & Flannery 1973). Evolution begins at zero-age main sequence (ZAMS) and continues to a user-specified age. The initial mass, M , angular velocity Ω and hydrogen and heavy element abundances X and Z are also set by the user. The models calculated here are $1M_{\odot}$ and $2M_{\odot}$ ZAMS models with solar elemental abundances and rotation rates ranging from $\Omega/\Omega_K = 0 - 0.25$, where $\Omega_K = \sqrt{GM/R^3}$ and R is the stellar radius. A selection of the models calculated is given in Table 1.

The effects of rotation were then included to second order in rotational velocity, Ω . In particular, the stellar structure is no longer spherically symmetric but oblate due to the centrifugal force. We therefore perform a transformation of the coordinate system $(r, \theta, \phi) \rightarrow (x, \theta, \phi)$, from a system of shells of constant radius, r , to shells of constant pressure, chosen such that $x = R$ maps the surface of the star which can now be treated as a surface in hydrostatic equilibrium. The new radial coordinate x takes the form

$$x = [1 + h_{\Omega}(r)P_2(\cos\theta)]r, \quad (1)$$

where h_{Ω} is the transformation coefficient and $P_2(\cos\theta) = \frac{3\cos^2\theta - 1}{2}$ the $\ell = 2$ Legendre polynomial. This can be inverted to give, to order Ω^2

$$r = [1 - h_{\Omega}(x)P_2(\cos\theta)]x. \quad (2)$$

We define a function $u = h_{\Omega}x$ such that u satisfies the following second order differential equation:

$$\mathcal{K}u = \mathcal{G}(x), \quad (3)$$

where

$$\mathcal{K} \equiv \frac{d^2}{dx^2} + \left(\frac{8\pi x^2 \rho_0}{Mq_0} - \frac{2}{x} \right) \frac{d}{dx} - \frac{4}{x^2}, \quad (4)$$

$$\mathcal{G}(x) = \frac{4\pi x^4 \rho_0}{GM^2 q_0^2} \left(f_{r2} - \frac{d}{dx}(x f_{\theta 2}) \right) + \frac{6x}{GMq_0} - \frac{1}{GMq_0} \frac{d}{dx} \left(x^2 \frac{d}{dx}(x f_{\theta 2}) \right), \quad (5)$$

and $f_{r,0} = -\frac{2}{3}\Omega^2 x$, $f_{r,2} = \frac{2}{3}\Omega^2 x$, $f_{\theta 2} = \frac{1}{3}\Omega^2 x$ and $q_0 = m/M$ is the fractional mass interior to a radius x . Boundary conditions for this system are

$$u \text{ regular as } x \rightarrow 0 \\ u' + \frac{u}{x} = -\frac{x^3}{GM} \left(x \frac{d}{dx}(f_{\theta 2}) + 4f_{\theta 2} \right) \quad \text{at } x = R.$$

The surface boundary condition is found by matching the gravitational potential Φ_0 onto the vacuum potential for $x > R$.

This change in coordinates leads to a change in all variables with a radial dependence such that e.g. $\rho_0(x) = \rho_0(r) + \rho_{\Omega}(r)P_2(\cos\theta)$, where the subscript “0” represents the equilibrium quantity, with similar expressions for $p_0(x)$ and $c_0(x)$.

Table 1. Model parameters.

M/M _⊙	Age (Gyr)	Ω/Ω _K	Ω (rad.s ⁻¹)	R/R _⊙	L/L _⊙	T _{eff} (K)	h _Ω (R)
1.00	0.00	0.0	0.00	0.89	0.69	5573.9	0.00
1.00	0.00	2.0×10 ⁻⁵	1.50×10 ⁻⁸	0.89	0.69	5573.9	1.40×10 ⁻¹⁰
1.00	0.00	2.0×10 ⁻⁴	1.50×10 ⁻⁷	0.89	0.69	5573.9	1.40×10 ⁻⁸
1.00	0.00	2.0×10 ⁻³	1.50×10 ⁻⁶	0.89	0.69	5573.9	1.40×10 ⁻⁶
1.00	0.00	2.0×10 ⁻²	1.50×10 ⁻⁵	0.89	0.69	5573.5	1.40×10 ⁻⁴
1.00	0.00	2.0×10 ⁻¹	1.49×10 ⁻⁴	0.89	0.67	5534.6	1.44×10 ⁻²
2.00	0.00	0.0	0.00	1.60	17.30	9307.87	0.00
2.00	0.00	2.0×10 ⁻⁵	8.76×10 ⁻⁹	1.60	17.30	9307.87	1.35×10 ⁻¹⁰
2.00	0.00	2.0×10 ⁻⁴	8.76×10 ⁻⁸	1.60	17.30	9307.87	1.35×10 ⁻⁸
2.00	0.00	2.0×10 ⁻³	8.76×10 ⁻⁷	1.60	17.30	9307.86	1.35×10 ⁻⁶
2.00	0.00	2.0×10 ⁻²	8.76×10 ⁻⁶	1.60	17.30	9307.18	1.35×10 ⁻⁴
2.00	0.00	2.0×10 ⁻¹	8.61×10 ⁻⁵	1.62	17.20	9240.81	1.39×10 ⁻²

3 PULSATION MODE CALCULATIONS

3.1 Perturbative analysis

In order to calculate perturbative frequencies we follow closely the method of Gough & Thompson (1990). The perturbation equation, to order Ω², can be written:

$$\mathcal{L}\vec{\xi} + \rho_0\omega^2\vec{\xi} = \omega\mathcal{M}\vec{\xi} + \mathcal{N}\vec{\xi} \quad (6)$$

where,

$$\begin{aligned} \mathcal{L}\vec{\xi} &= -\vec{\nabla} \left[(p_0 - \rho_0 c_0^2) \vec{\nabla} \cdot \vec{\xi} - \vec{\xi} \cdot \vec{\nabla} p_0 \right] + p_0 \vec{\nabla} (\vec{\nabla} \cdot \vec{\xi}) \\ &\quad - \vec{\xi} \cdot \vec{\nabla} (\ln \rho_0) \nabla p_0, \\ \mathcal{M}\vec{\xi} &= -2i\rho_0 \vec{v} \cdot \vec{\nabla} \vec{\xi}, \\ \mathcal{N}\vec{\xi} &= \rho_0 \left[-\vec{\xi} \cdot \vec{\nabla} (\vec{v} \cdot \vec{\nabla} \vec{v}) + (\vec{v} \cdot \vec{\nabla})^2 \vec{\xi} \right]. \end{aligned} \quad (7)$$

Here p_0 , ρ_0 and c_0 are the equilibrium pressure, density and sound speed respectively, ω is the angular pulsation frequency and \vec{v}_0 the velocity field resulting from rotation. $\vec{\xi}$ is the Lagrangian displacement and is defined such that

$$\vec{\xi}_{nlm} = \left(\xi(r) Y_\ell^m(\theta, \phi), \eta(r) \frac{\partial Y_\ell^m(\theta, \phi)}{\partial \theta}, \frac{\eta(r)}{\sin \theta} \frac{\partial Y_\ell^m(\theta, \phi)}{\partial \phi} \right) \quad (8)$$

where ξ , η are the radial and horizontal amplitude functions respectively and Y_ℓ^m is the spherical harmonic for a mode of degree ℓ , radial order n and azimuthal order m . We choose to normalise Y_ℓ^m such that

$$\int_0^{2\pi} \int_0^\pi |Y_\ell^m(\theta, \phi)|^2 \sin \theta d\theta d\phi = 1, \quad (9)$$

and we normalise $\xi(r)$ such that $\xi(R) = 1$.

The structural changes of the equilibrium model resulting from rotation cause perturbations to the eigenfunction $\vec{\xi}$ and to the function $\mathcal{L}\vec{\xi}$, denoted respectively by $\vec{\xi}_1$ and $\mathcal{L}_\Omega\vec{\xi}$. For further details we refer the reader to Gough & Thompson (1990). These perturbation quantities are substituted into equation (6) and we linearise the resulting expression to second order in rotational velocity Ω. This leads to the following expression for the oscillation frequency, valid to second order in Ω:

$$\begin{aligned} \omega_{nlm} &= \omega_0 + \omega_{\Omega 1} + (2I\omega_0)^{-1} \langle \vec{\xi}_0^* \cdot (\mathcal{N}_0 - \mathcal{L}_\Omega - \rho_\Omega \omega_0^2) \vec{\xi}_0 \rangle \\ &\quad - \omega_{\Omega 1}^2 (2\omega_0)^{-1} - \omega_{\Omega 1} I^{-1} \langle \rho_0 \vec{\xi}_0^* \cdot \vec{\xi}_1 \rangle \end{aligned}$$

$$\begin{aligned} &+ (2I)^{-1} \langle \vec{\xi}_0^* \cdot \mathcal{M}_0 \vec{\xi}_1 \rangle \\ &+ \omega_{\Omega 1} (2I\omega_0)^{-1} \langle \vec{\xi}_0^* \cdot \mathcal{M}_0 \vec{\xi}_0 \rangle, \end{aligned} \quad (10)$$

where $\langle \dots \rangle = \int_0^{2\pi} \int_0^\pi \int_0^R \dots x^2 \sin \theta dx d\theta d\phi$ is, to first order, the volume integral over the interior of the star. ω_0 is the unperturbed oscillation frequency,

$$I = \int_0^R \rho_0 x^2 [\xi^2 + \ell(\ell+1)\eta^2] dx, \quad (11)$$

and $\omega_{\Omega 1}$ contains the terms to first order in Ω and can be expressed as:

$$\omega_{\Omega 1} = \frac{m}{I} \int_0^R \Omega \rho_0 x^2 [(\xi - \eta)^2 + (\ell(\ell+1) - 2)\eta^2] dx. \quad (12)$$

The ADIPLS adiabatic pulsation package (Christensen-Dalsgaard 2008a) was then modified to include second order rotational effects, and subsequently used to calculate perturbative frequencies.

3.2 Two-dimensional calculations

In order to carry out the two-dimensional pulsation calculations, we used the same approach as in Reese et al. (2009). The pulsation equations are expressed in terms of a new coordinate system which follows the shape of the star, then projected onto the spherical harmonic basis, and finally solved using the pulsation code TOP (Two-dimensional Oscillation Program, Reese et al. 2009).

The new coordinate system can be represented by (ζ, θ, ϕ) where ζ is the radial coordinate, θ the colatitude, and ϕ the longitude. The relationship between ζ and r , the distance from the origin, is given by the following two equations:

$$r(\zeta, \theta) = (1 - \epsilon)\zeta + \frac{5\zeta^3 - 3\zeta^5}{2} (R_s^*(\theta) - 1 + \epsilon), \quad (13)$$

$$\begin{aligned} r(\zeta, \theta) &= 2\epsilon + (1 - \epsilon)\zeta \\ &\quad + (2\zeta^3 - 9\zeta^2 + 12\zeta - 4) (R_s^*(\theta) - 1 - \epsilon), \end{aligned} \quad (14)$$

where $\epsilon = 1 - \frac{R_{\text{pol}}^*}{R}$, $R_s^*(\theta) = \frac{R^*}{R} - P_2(\cos \theta) \frac{R^* h_\Omega(R^*)}{R}$, R_{pol}^* is the polar radius at the last grid point and R^* the radial coordinate at the last grid point. The first equation applies to the first domain, *i.e.* for $\zeta \in [0, 1]$, which corresponds to

the star. It must be noted that contours of constant x and ζ values do not in general coincide, except at the last grid point where $x = R^*$ and $\zeta = 1$, because only the former corresponds to isobars. As a result, the model must be interpolated onto this new grid. The second equation applies to the second domain, *i.e.* for $\zeta \in [1, 2]$, which lies outside the star and in which only the perturbation to the gravitational potential is used. This coordinate system ensures that the standard regularity conditions can be used in the centre since it behaves like the spherical coordinate system in the centre, and it allows the use of simple boundary conditions both on the stellar surface for the Lagrangian displacement and pressure fluctuations, and on the outer boundary of the second domain for the perturbation to the gravitational potential.

The pulsation equations are expressed in terms of the Lagrangian displacement, $\vec{\xi}$:

$$0 = \rho + \vec{\nabla} \cdot (\rho_0 \vec{\xi}), \quad (15)$$

$$0 = [-\omega + m\Omega]^2 \rho_0 \vec{\xi} - 2i[-\omega + m\Omega] \rho_0 \vec{\Omega} \times \vec{\xi} - \vec{\nabla} p + \rho \vec{g}_{\text{eff}} - \rho_0 \vec{\nabla} \Psi, \quad (16)$$

$$0 = p + \vec{\xi} \cdot \vec{\nabla} p_0 - c_0^2 (\rho + \vec{\xi} \cdot \vec{\nabla} \rho_0), \quad (17)$$

$$0 = \Delta \Psi - \Lambda \rho, \quad (18)$$

where ρ , p and Ψ are the density, pressure and gravitational potential fluctuations. This is the same set of equations as what is given in the appendix of Reese et al. (2009) except that there is no gradient of the rotation rate, since the rotation profile is uniform, and each occurrence of ω has been replaced by $-\omega$, so as to ensure that prograde modes correspond to positive values of m , the azimuthal order. Furthermore, in order to increase the accuracy of the calculations, the effective gravity has been calculated from the gradient of the total potential rather than from the gradient of the pressure divided by the density. For explicit expressions in terms of the spheroidal coordinate system, we refer the reader to Reese et al. (2009).

Calculating pulsation modes in models based on the ASTEC code (Christensen-Dalsgaard 2008b) is similar to calculating modes in models based on the Self-Consistent Field (SCF) method (MacGregor et al. 2007), although there are some noteworthy differences. ASTEC models include atmospheres which means that the associated radial grids become very dense near the surface. As a result, care must be taken when expressing the radial differential operator in algebraic form. For instance, using the fourth order finite difference implemented in Reese et al. (2009) leads to numerically unstable behaviour. This has been replaced with a more stable version of fourth order finite differences, in which the differential equations are solved on carefully chosen intermediate grid points.

4 VALIDITY DOMAINS FOR PERTURBATIVE CALCULATIONS

Before establishing validity domains for second order perturbative methods, it is important to compare the two methods for non-rotating (or nearly non-rotating) stars. Differences arise from the different formulations of the pulsation

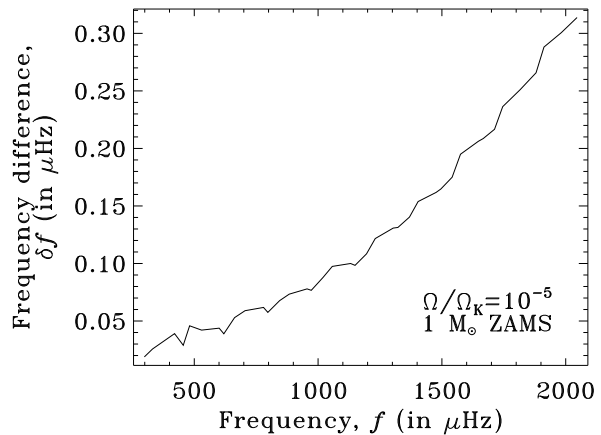


Figure 1. A comparison of $m = 0$ modes for a $1 M_{\odot}$ model rotating at $\Omega = 10^{-5} \Omega_K$. The radial orders are $n = 1, 10$ and the harmonic degrees $\ell = 0, 3$. These differences are larger than $0.08 \mu\text{Hz}$, the error bar on a CoRoT long run, and must therefore be taken into account when constructing validity domains.

equations and should be correctly characterised before proceeding to establish validity domains. Figure 1 shows the differences between $m = 0$ modes calculated with the two methods. Although this error is small, it is larger than the error bar from a CoRoT long run and should therefore be taken into account when constructing validity domains.

Figure 2 shows a comparison between the two methods for three different error bars. The first two correspond to a long and short CoRoT run and the third corresponds to 2.3 days of observation. The radial orders of the modes are $n = 1-10$, the harmonic degrees $\ell = 0-3$ and the azimuthal orders $m = -l$ to l . Frequency multiplets calculated using perturbative theory were shifted using the differences which are plotted in Fig. 1. This leads to somewhat larger and more realistic validity domains, especially for the smallest error bar. Based on these validity domains, non-perturbative effects will start to play an important role beyond $v_{\text{eq}} = 30 \text{ km.s}^{-1}$ for a long run, and $v_{\text{eq}} = 50 \text{ km.s}^{-1}$ for a short run, in a $1 M_{\odot}$ star. However, given that solar-like pulsators tend to oscillate with radial orders between 15 and 25, these limits are expected to be lower, as based on the trends which can be seen in Fig. 2.

If the perturbative frequencies are replaced with polynomial fits to the non-perturbative frequencies, similar validity domains are obtained, as can be seen in Fig. 3. This comparison shows that there is a good agreement between the polynomial coefficients and the coefficients deduced from perturbative theory, thus providing a further check that both the perturbative and two-dimensional approach agree at low rotation rates.

It is then interesting to compare these validity domains with those obtained from polytropic models. Figure 4 shows such a comparison. It includes the validity domain for $N = 3$ and $N = 1.5$ polytropic models and compares them with that of the $1 M_{\odot}$ ZAMS model using the $0.6 \mu\text{Hz}$ error bar. The polytropic models are scaled so as to have the

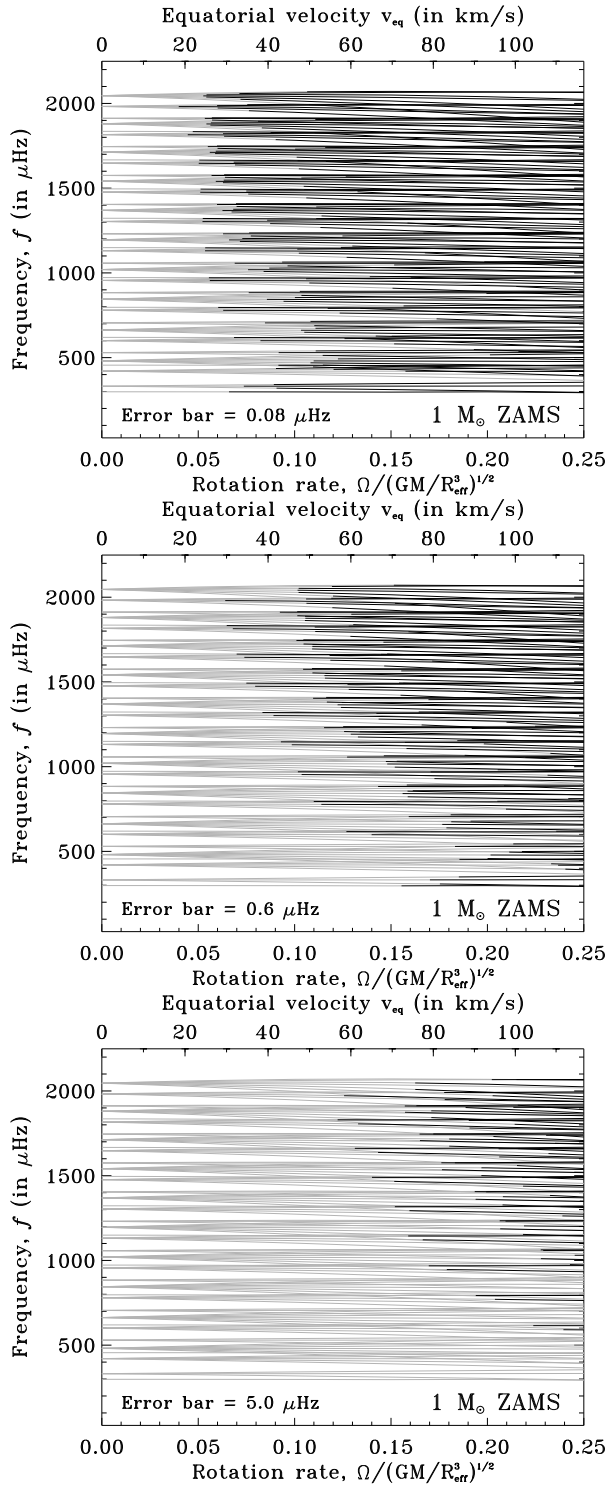


Figure 2. Validity domains for second order perturbative frequencies of $1 M_{\odot}$ ZAMS models for three different error bars, the first two corresponding to CoRoT error bars. These figures are analogous to Fig. 4 of Reese et al. (2006), which were established for an $N = 3$ polytropic model.

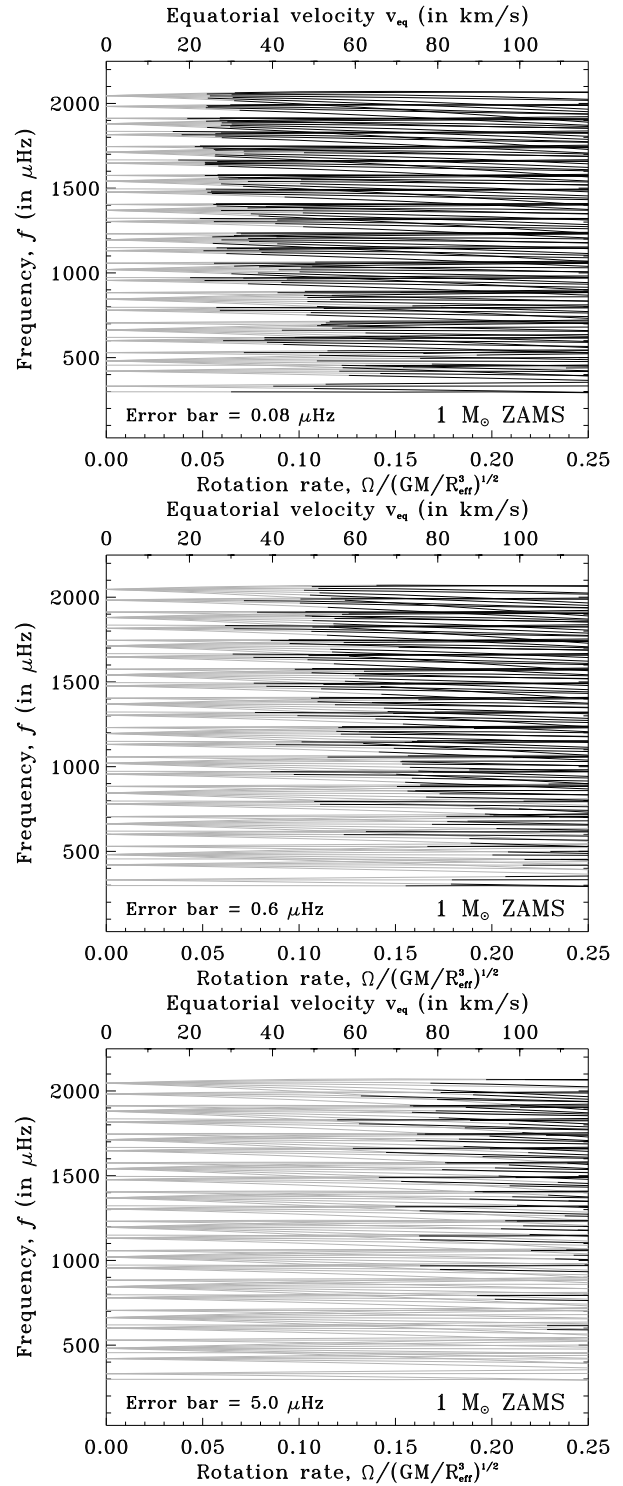


Figure 3. Same as Fig. 2 except that the perturbative frequencies have been replaced with second order polynomial fits to the non-perturbative frequencies.

same mass and approximately the same radii² as the $1 M_{\odot}$ ZAMS model. In order to superimpose the different valid-

² The polar and equatorial radii were made to satisfy $\frac{R_{\text{pol}} + R_{\text{eq}}}{2} = 0.89 R_{\odot}$, which is approximately true of the $1 M_{\odot}$ ZAMS model.

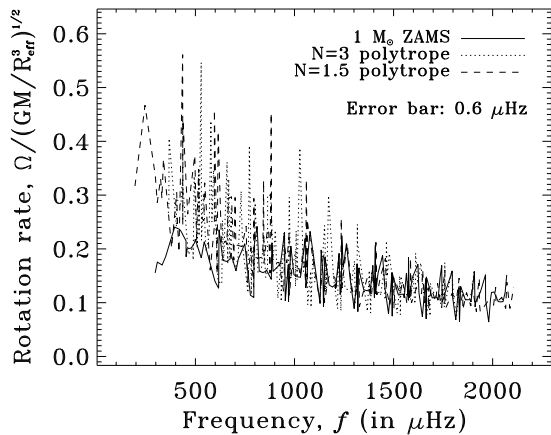


Figure 4. Comparison between the validity domains for two polytropic models and the $1 M_{\odot}$ ZAMS model, for the $0.6 \mu\text{Hz}$ error bar. The threshold separating the regions where perturbative methods are valid and not valid is plotted so as to allow the superposition of the different domains.

ity domains, we have simply plotted the threshold between the region where the perturbative approach is valid, and the region where a two-dimensional calculation becomes necessary. As can be seen from the figure, the validity domains are quite similar. At high frequencies, they follow the same tendency as a function of frequency and have a similar spread around the mean value. At low frequencies, the threshold for the $1 M_{\odot}$ model seems to be, on average, lower than that of the polytropic models. This effect is, however, likely to be an artifact due to the cutoff at $\Omega = 0.25 \Omega_K$ for the $1 M_{\odot}$ frequency calculations (see Fig. 2).

5 CLOSE FREQUENCY PAIRS

In Espinosa et al. (2004), it was pointed out that adjacent frequencies within a multiplet tend to pair up and come close together, except for the most retrograde mode (*i.e.* $l = -|m|$ sectoral mode). It was then suggested that this phenomena could explain the close frequency pairs observed in Breger & Bischof (2002) (see also Breger & Pamyatnykh 2006b and Breger & Pamyatnykh 2006a). A similar pairing up of modes also occurs for the frequencies in Reese et al. (2006) as well as the non-perturbative frequencies presented here. In what follows, we will consider $2 M_{\odot}$ ZAMS models, as this is more representative of δ Scuti stars. The second half of Table 1 gives the characteristics for a selection of these models.

Figure 5 shows four sets of $l = 2$ multiplets calculated using both perturbative and two-dimensional calculations. As can be seen in the figures, only the two-dimensional calculations lead to this behaviour. The perturbative calculations produce, instead, spacings which decrease uniformly when going from the most retrograde to the most prograde mode. However, the effects of avoided crossings have not been included in the perturbative calculations, so it remains to be seen whether including this effect can also produce a pairing up of adjacent frequencies.

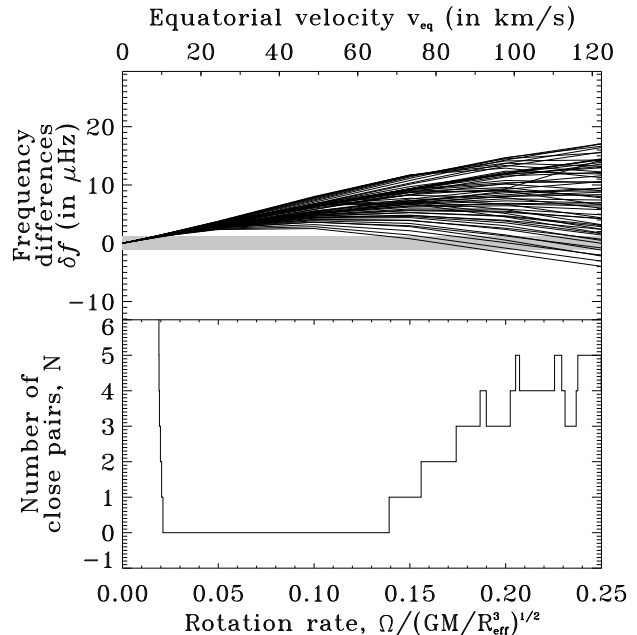


Figure 6. *Upper panel:* frequency differences between adjacent modes in the $l = 1 - 3$ frequency multiplets of $2 M_{\odot}$ models, as a function of the rotation rate. The frequency span of the spectrum is approximately $250 - 1060 \mu\text{Hz}$. The grey band in the middle corresponds to differences which are less than $0.1 c/d$. *Lower panel:* number of frequency differences below $0.1 c/d$ as a function of the rotation rate. This number is generally quite low except for slow rotation rates, where the average spacing between frequencies in a multiplet is comparable to $0.1 c/d$.

It is then interesting to investigate whether this effect could explain the close frequency pairs observed in Breger & Pamyatnykh (2006b). In Fig. 6, we compare the frequency differences of mode pairs to a frequency separation of $0.1 c/d$ (*i.e.* $1.1574 \mu\text{Hz}$), a typical threshold for observed frequency pairs. As can be seen from the upper panel, these differences remain larger on average than $0.1 c/d$. The lower panel shows the number of sufficiently close frequencies as a function of the rotation rate. As can be seen, this number is not very large for any given rotation rate, except when the rotation rate is around or below $0.1 c/d$. However, 18 close frequency pairs were observed in FG Vir (Breger & Pamyatnykh 2006a), and its equatorial velocity is estimated to be $66 \pm 16 \text{ km.s}^{-1}$, as based on the modelling of line profile variations (Zima et al. 2006). As a result, the pairing up of adjacent modes in frequency multiplets do not seem to account for close frequency pairs in δ Scuti stars.

Of course, it is always possible to look at all of the frequency differences for a given spectrum. This approach has been used by Lenz, Pamyatnykh & Breger (2008) to study 3 δ Scuti stars, including FG Vir. Here, we will push the analysis slightly further by looking at how the number of close frequency pairs depends on the rotation rate. Figure 7 shows the number of close frequency pairs as a function of the rotation rate, as well as where they occur. The dashed

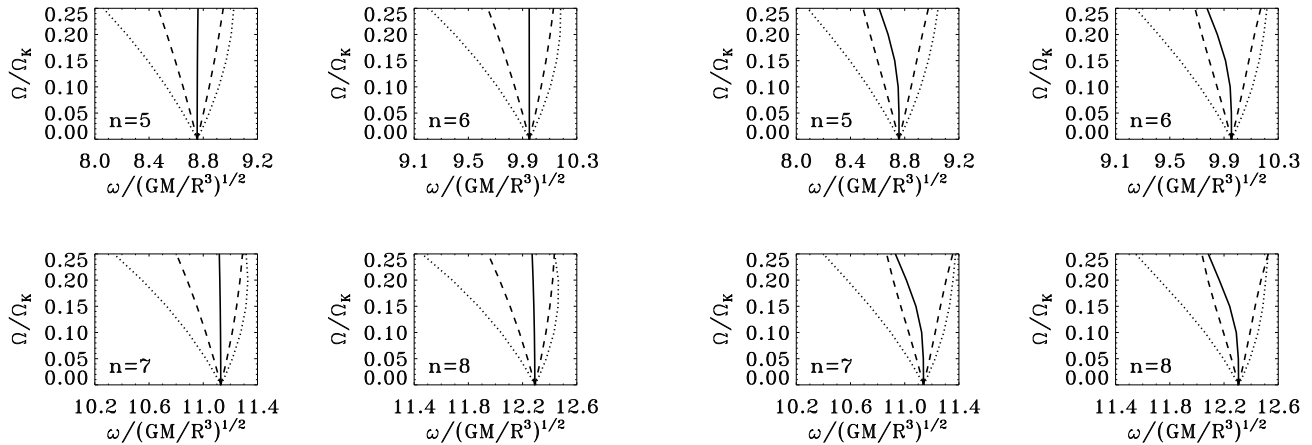


Figure 5. Four $\ell = 2$ multiplets calculated using perturbative (*left*) and two-dimensional (*right*) calculations in $2 M_{\odot}$ models. Frequencies only pair up in the two-dimensional calculations. In the perturbative case, the spacings decrease uniformly when going from the most retrograde to the most prograde mode.

line in the lower panel gives the expected number of pairs, $N_{\text{exp.}}$, as based on a Poisson distribution:

$$N_{\text{exp.}} = (N_{\text{mode}} - 1) \left[1 - \exp\left(-\frac{(N_{\text{mode}} - 1) \delta f}{\Delta f}\right) \right] \quad (19)$$

where N_{mode} is the number of modes in the spectrum, Δf the frequency span of the spectrum, and δf the target frequency separation (*i.e.* 0.1 c/d). At a sufficient rotation rate, the average number of close frequency pairs matches $N_{\text{exp.}}$ indicating that the spectrum is behaving like a Poisson distribution. As was pointed out by Lignières & Georgot (2008) and Lignières & Georgot (2009), the frequency spectrum of rapidly rotating stars is subdivided into classes of regular modes, such as these low degree modes, and chaotic modes, the frequencies of which follow Poisson and Wigner distributions respectively, provided there are no selection effects.

The number of close frequency pairs is much higher than in the previous case and higher than the number of pairs observed in FG Vir. However, Fig. 7 is based on 160 frequencies, whereas there are 67 independent frequencies detected in FG Vir. Applying Eq. (19) to FG Vir’s frequency spectrum yields 10.4 close frequency pairs, which is slightly over half the number of observed close frequency pairs in this star. Also, as pointed out in Lenz et al. (2008), there are 7 frequency pairs where the separation is below 0.01 c/d. Equation (19) would yield 1.12 very close frequency pairs for FG Vir. Furthermore, according to Breger & Pamyatnykh (2006a), close frequency pairs seem to cluster around radial modes, whereas a number of pairs in Fig. 7 are close to the midpoints between consecutive radial modes. Hence, an astrophysical origin is still needed to account for this phenomena.

An interesting feature appears in Fig. 7. Between approximately $0.02 \Omega_K$ and $0.05 \Omega_K$, few frequency pairs are detected. A simple explanation is that the rotation rate is sufficient to keep individual multiplet components far enough apart, but too small to cause frequency multiplets to overlap. Of course, including modes with higher ℓ values would probably reduce this gap by introducing new multi-

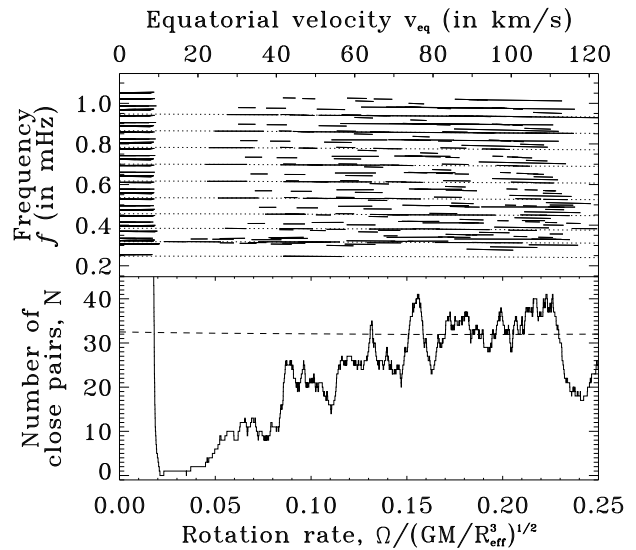


Figure 7. *Upper panel:* close frequency pairs in $2 M_{\odot}$ models as a function of the rotation rate for the frequency spectrum ($n = 1 - 10$, $l = 0 - 3$, $m = -l$ to l). The horizontal dotted lines show the location of radial modes. *Lower panel:* number of close frequency pairs as a function of the rotation rate. The dashed line shows the number of close frequency pairs that is expected for a Poisson distribution.

plets into the frequency spectrum. However, as was pointed out by Lignières et al. (2006) and Lignières & Georgot (2009), cancellation effects for such modes are more effective at lower rotation rates, *i.e.* where close frequencies pairs are lacking. Table 2 gives a list of δ Scuti stars where close frequencies have been reported. Interestingly, none of the stars fall in this gap. Of course, a larger number of stars would need to be analysed to see whether this gap remains or whether it is simply due to poor statistics. Furthermore, some of the stars in Table 2, such as BI CMi (Breger et al. 2002), BV Cir (Mantegazza, Poretti & Zerbi 2001) and 44

Star	HD number	$v \cdot \sin i$ (km.s ⁻¹)	Reference
BI CMi	66853	76 ± 1	Breger et al. (2002)
XX Pyx		52 ± 2	Handler et al. (1997)
V509 Per	18878	134	Bush & Hintz (2008)
4 CVn	107904	112 ± 3 ^a	Bush & Hintz (2008)
FG Vir	106384	21.6 ± 0.3 ^b	Zima et al. (2006)
BV Cir	132209	96.5 ± 1	Mantegazza et al. (2001)
BW Cnc	73798	200 ± 11	Fossati et al. (2008)
44 Tau	26322	2 ± 1 ^c	Zima et al. (2007)

Table 2. Projected equatorial velocities of δ Scuti stars with observed close frequency pairs (this list is based on Breger & Bischof 2002 and Lenz et al. 2008). The first two columns identify the star. The third and fourth columns give the projected equatorial velocity and the reference where this velocity is obtained. ^a Bush & Hintz (2008) give a list of several values. The value given here is the average plus or minus the standard deviation. ^b Although the projected equatorial velocity is small, Zima et al. (2006) estimate that the true equatorial velocity is 66 ± 16 km.s⁻¹. ^c Zima et al. (2007) estimate that the true equatorial velocity is 3 ± 2 km.s⁻¹.

Tau (Zima et al. 2007), are evolved. Consequently, their pulsation spectra are likely to contain acoustic, gravity (or gravito-inertial) and possibly mixed modes.

6 CONCLUSION

In this study, the effects of stellar rotation on acoustic pulsation frequencies have been investigated using a second order perturbative and a two-dimensional approach. A comparison of the two shows that perturbative methods are valid for equatorial velocities up to 30 and 50 km.s⁻¹ for a CoRoT long and short run, respectively. The associated validity domains closely match the domains previously obtained in Reese et al. (2006) for polytropic models. These results show that perturbative methods, which are simpler to work with and less demanding numerically, will remain useful for a number of stars. Nonetheless, various qualitative and quantitative differences appear between this approach and two-dimensional calculations at sufficient rotation rates. Among these is the pairing up of adjacent modes in frequency multiplets. This phenomena, first noted in Espinosa et al. (2004), also shows up in the two-dimensional calculations presented here but not in the second order perturbative calculations, in which the spacing between consecutive modes varies monotonically. The cause of this pairing up remains a mystery, given that different modes in a multiplet are not coupled due to their differing azimuthal orders.

The case of observed close frequency pairs is then discussed. In particular, it is shown that adjacent mode pairs in frequency multiplets do not come close enough together to provide a likely explanation, as opposed to what was previously suggested (Espinosa et al. 2004). A systematic search for all of the close frequencies pairs in the calculated spectra was then carried out. Results showed that at sufficient rotation rates, the number of close pairs of low degree acoustic modes matched what is expected based on a Poisson distribution. Even then, this does not match the number and distribution of close pairs observed in stars like FG Vir

thereby favouring an astrophysical origin to the phenomena. At lower rotation rates, where frequency multiplets do not overlap, a lack of close frequency pairs is observed in the calculated spectra, except at the lowest rotation rates where the rotational shift is small. Delta Scuti stars currently reported as having close frequency pairs do not lie in this interval, but a more systematic study is required to see to what extent this is due to poor statistics, and to see what effects including gravity type modes has for more evolved stars.

ACKNOWLEDGEMENTS

The authors wish to thank the referee for useful comments which have helped to clarify the manuscript and improve the scientific discussion. DRR gratefully acknowledges support from the CNES (“Centre National d’Etudes Spatiales”) through a postdoctoral fellowship, the UK Science and Technology Facilities Council through grant ST/F501796/1, and the European Helio- and Asteroseismology Network (HELAS), a major international collaboration funded by the European Commission’s Sixth Framework Programme. This research has made use of the SIMBAD database, operated at CDS, Strasbourg, France.

References

- Breger M., Bischof K. M., 2002, *A&A*, 385, 537
- Breger M. et al. 2002, *MNRAS*, 329, 531
- Breger M., Pamyatnykh A. A., 2006a, *MNRAS*, 368, 571
- Breger M., Pamyatnykh A. A., 2006b, *Memorie della Societa Astronomica Italiana*, 77, 295
- Bush T. C., Hintz E. G., 2008, *Astr. J.*, 136, 1061
- Christensen-Dalsgaard J., 2008a, *ApSS*, 316, 113
- Christensen-Dalsgaard J., 2008b, *ApSS*, 316, 13
- Clement M. J., 1981, *ApJ*, 249, 746
- Dziembowski W. A., Goode P. R., 1992, *ApJ*, 394, 670
- Eggleton P. P., Faulkner J., Flannery B. P., 1973, *A&A*, 23, 325
- Espinosa F., Pérez Hernández F., Roca Cortés T., 2004, in *ESA SP-559: SOHO 14 Helio- and Asteroseismology: Towards a Golden Future Oscillation Modes in Axially Symmetric Stars*. pp 424–427
- Fossati L., Bagnulo S., Landstreet J., Wade G., Kochukhov O., Monier R., Weiss W., Gebran M., 2008, *A&A*, 483, 891
- Gough D. O., Thompson M. J., 1990, *MNRAS*, 242, 25
- Handler G. et al. 1997, *MNRAS*, 286, 303
- Iglesias C. A., Rogers F. J., 1996, *ApJ*, 464, 943
- Karami K., Christensen-Dalsgaard J., Pijpers F. P., Goupil M.-J., Dziembowski W. A., 2005, *astro-ph/0502194*
- Kjeldsen H., Christensen-Dalsgaard J., Handberg R., Brown T. M., Gilliland R. L., Borucki W. J., Koch D., 2010, *astro-ph.SR/1007.1816*
- Kurucz R. L., 1991, in *NATO ASIC Proc. 341: Stellar Atmospheres - Beyond Classical Models New opacity calculations*. p. 441
- Lenz P., Pamyatnykh A. A., Breger M., 2008, *Journal of Physics Conference Series*, 118, 012063
- Lignières F., Georgeot B., 2008, *Phys. Rev. E*, 78, 016215
- Lignières F., Georgeot B., 2009, *A&A*, 500, 1173

- Lignières F., Rieutord M., Reese D., 2006, *A&A*, 455, 607
Lovekin C. C., Deupree R. G., 2008, *ApJ*, 679, 1499
MacGregor K. B., Jackson S., Skumanich A., Metcalfe T. S., 2007, *ApJ*, 663, 560
Mantegazza L., Poretti E., Zerbi F. M., 2001, *A&A*, 366, 547
Michel E. et al. 2008, *Communications in Asteroseismology*, 156, 73
Ouazzani R.-M., Goupil M.-J., Dupret M.-A., Reese D., 2009, *Communications in Asteroseismology*, 158, 283
Reese D., Lignières F., Rieutord M., 2006, *A&A*, 455, 621
Reese D. R., MacGregor K. B., Jackson S., Skumanich A., Metcalfe T. S., 2009, *A&A*, 506, 189
Saio H., 1981, *ApJ*, 244, 299
Soufi F., Goupil M.-J., Dziembowski W. A., 1998, *A&A*, 334, 911
Suárez J. C., Goupil M. J., Reese D. R., Samadi R., Lignières F., Rieutord M., Lochard J., 2010, *ApJ*, 721, 537
Yoshida S., Eriguchi Y., 2001, *MNRAS*, 322, 389
Zima W., Lehmann H., Stütz C., Ilyin I. V., Breger M., 2007, *A&A*, 471, 237
Zima W. et al. 2006, *A&A*, 455, 235